Analytical Load-Moment Interactions of Shape Modified Square Hollow RC Columns Subjected to Bi-Axial Eccentric Loading: A Parametric Study

Mohammed Tareq Jameel
Department of Physics, College of Education, Al-Iraqia University, Baghdad, Iraq
mohammed.t.jameel@aliraqia.edu.iq (corresponding author)

Received: 17 February 2025 | Revised: 17 March 2025 | Accepted: 28 March 2025

 DOI: https://doi.org/10.48084/etasr.10553

ABSTRACT

This paper presents analytical load-moment interactions for shape modified square hollow Reinforced Concrete (RC) columns into circular and wrapped with Fiber Reinforced Polymer (FRP) under biaxial eccentric loadings. The analysis is performed using strip integration methods along with theoretical stress and strain constitutive models of concrete, adopted from the existing studies. The theoretical predictions show good agreement with the experimental results available in the literature for both biaxially loaded FRP-wrapped square solid RC columns and uniaxially loaded FRP-wrapped, shape-modified square hollow RC columns, in terms of axial load capacity and corresponding bending moment. The effect of the number of FRP wrapping layers, compressive strength, and hole size were investigated for the biaxially loaded shape modified square hollow RC columns. Four regions are determined to form the interaction diagram, including: pure compression, balance point, pure tension and any other point. The results reveal that higher axial loads and bending moments can be achieved with an increased number of FRP layers and greater concrete strength. Conversely, a larger hole size reduces confinement efficiency, and overall FRP confinement effectiveness is diminished as biaxial eccentricity increases.

Keywords-hollow columns; confinement; shape modification; biaxial eccentricity; concrete segment

I. INTRODUCTION

Tall bridges and piers commonly utilize hollow concrete columns as compression members. Compared to solid columns, hollow columns offer a lower weight to stiffness ratio due to the presence of a central void. This central hole helps reduce temperature gradients caused by the heat of hydration across the concrete wall thickness, thereby minimizing shrinkage cracks in the concrete [1]. However, the presence of the central hole can result in poor ductility [1, 2].

Wrapping circular and square hollow concrete columns can increase the strength and ductility under different loading conditions [2-4]. Nevertheless, the effectiveness of FRP confinement in hollow RC columns is affected by several parameters, such as the strength of the unconfined concrete, the radius of the column corners, the number of FRP layers applied, and the dimensions of the central void. The confinement efficiency increases with the increased number of FRP wrapping layers and unconfined concrete strength [3, 5]. Furthermore, the confinement efficiency decreases with the increased size of the inner hole [2, 5]. Conversely, confinement efficiency tends to decrease as the size of the central void increases [2, 5]. It has also been observed that confinement becomes more effective with increasing corner radii, reaching its peak for circular cross-sections [3]. One approach to enhance FRP confinement is to round the column corners, as the efficiency increases with larger corner radii [5]. The technique of modifying the shape of square solid RC columns into circular ones by attaching plain concrete segments on the sides can eliminate the effect of corner sharpness and enhance the performance of CFRP confinement [6-8]. The shape modification technique can also increase the efficiency of CFRP confinement for square hollow concrete specimens subjected to concentric and uniaxial eccentric loads [4].

The types of loads applied to a structural member depend on its position within the structure. Columns may be subjected to either concentric axial loads or eccentric loads, with the latter inducing uniaxial bending moments. In certain cases, depending on the location of the eccentric axial load relative to the cross-sectional axis, the resulting bending moment may be either uniaxial or biaxial, as illustrated in Figure 1. Interaction diagrams for axial load and bending moment in FRP-confined square and circular hollow RC columns under uniaxial eccentric loading have been widely reported in the literature [8]. However, only limited studies have addressed the axial load–bending moment interaction in FRP-wrapped, shape-modified square hollow RC columns under uniaxial eccentricity [4].

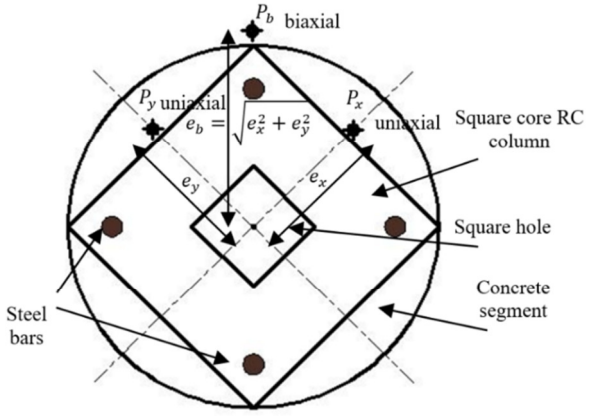

Fig. 1. Types of the eccentric applied axial load according to the position with respect to cross section's axis: e_x and e_y are uniaxial eccentricities, and $e_b = \sqrt{e_x^2 + e_y^2}$ is biaxial eccentricity.

When a shape-modified RC column is subjected to biaxial loading, the geometry of the core square concrete section and the arrangement of steel reinforcement remain unchanged. As a result, the core is capable of undergoing biaxial bending under eccentric loads.

To date, axial load–bending moment interactions for FRP-wrapped, shape-modified hollow RC columns under biaxial eccentric loading have not been examined in the literature. This gap forms the primary motivation for the present study.

The current paper presents a theoretical analysis of the biaxial load and corresponding biaxial bending moment in shape-modified square hollow RC columns, which are transformed into circular sections by attaching curved precast concrete segments to each side and subsequently wrapping them with FRP. The theoretical findings are validated against the experimental results reported in [4, 9].

II. ANALYTICAL CONSIDERATION

A. Confinement Modeling of Concrete

When FRP-wrapped columns are subjected to axial compression, the concrete begins to expand laterally due to Poisson's effect. As the loading progresses, the FRP wrapping resists this radial dilation, thereby enhancing the strength and ductility of the concrete, which is subjected to a triaxial state of stress. In hollow columns, however, the effectiveness of the FRP confinement is reduced due to the presence of the central void, which allows the concrete to expand freely toward the inner cavity. As a result, the concrete primarily experiences a biaxial stress state (circumferential and axial). Therefore, the presence of the inner void must be accounted for when modeling the behavior of FRP-wrapped hollow concrete columns. The behavior of shape-modified hollow columns is assumed to be similar to that of circular hollow columns, since experimental observations have shown no debonding between the square core and the added concrete segments at failure [4]. The confinement pressure of FRP resulting from dilation of concrete is passive, as the confinement increases with the increase in the axial compression. The effect of the hole on the confinement pressure was developed in [5] by proposing the hole ratio factor $\left(\beta = 1 - \frac{r_h^2}{R_c^2}\right)$, which is equal to 1 for a solid column. By introducing the hole effect into the confinement pressure in [10, 11], the confinement pressure $f_{Hconf.}$ of the hollow column can be determined as:

$$f_{Hconf.} = \frac{2(E_{frup}\, k_\varepsilon\, \varepsilon_{fcoup.})t}{2R_c}\beta \quad (1)$$

where E_{frup} denotes to the elastic modulus of FRP, t represents the FRP wrapping thickness, R_c and r_h refer to the radius of the circular section of the column and radius of inner hole, respectively, and k_ε denotes the efficiency factor of confinement strain, which was given a value of 0.586 [10]. Multiplying the FRP strain from the coupon test ($\varepsilon_{fcoup.}$) by the strain efficiency factor (k_ε) gives the real rupture strain of FRP (ε_{frup}).

Authors in [10] proposed a model, which is adopted in this study to calculate the confinement strength of hollow columns, based on the confinement pressure defined earlier in (1):

$$\frac{f'_{cch}}{f'_{co}} = 1 + k\, k_a\, \frac{f_{Hconf}}{f'_{co}} \quad (2)$$

where f'_{co} refers to the strength of unconfined concrete ,f'_{cch} refers to the ultimate compressive strength of confined concrete, as stated in [10], k is a constant used equal to 3.3, and k_a is the geometry shape factor proposed that is equal to 1 for circular cross section, while, for square cross-section with corner radius (R_{corn}) is:

$$k_a = \left(\frac{w}{h}\right)^2 \frac{1-\left((w-2R_{corn})^2 + \frac{(h-2R_{corn})^2}{3A_c}\right)-\rho_s}{1-\rho_s} \quad (3)$$

The ultimate compressive strain of hollow concrete can be calculated using modified Lam and Teng's [10] models as:

$$\varepsilon_{cuH} = \varepsilon_{co} k_{a\varepsilon}\left[k_c + 12\,\frac{f_{Hconf.}}{f'_{co}}(\varepsilon_{Hrr})^{0.45}\right] \quad (4)$$

$$\varepsilon_{Hrr} = \frac{\varepsilon_{h,rup}}{\varepsilon_{co}} \quad (5)$$

where k_c is a constant and is equal to 1.75 in this study, $\varepsilon_{h,rup}$ represents the hoop rupture strain of FRP, ε_{co} represents the axial strain of unconfined concrete, ε_{cuH} represents the confinement concrete strain at ultimate stress. $k_{a\varepsilon}$ is the geometry shape factor, which is equal to 1 for the circular cross section, while, for the square cross-section it is:

$$k_{a\varepsilon} = \left(\frac{w}{h}\right)^{0.5} \frac{1-\left((w-2R_{corn})^2 + \frac{(h-2R_{corn})^2}{3A_c}\right)-\rho_s}{1-\rho_s} \quad (6)$$

In this study, the axial stress–axial strain behavior of FRP-confined concrete is evaluated using the model developed in [10], formulated as:

$$f'_{chi} = \begin{cases} E_c\varepsilon_c - \frac{((E_c - E_{cc}))^2}{4f'_{co}}\varepsilon_c{}^2 \text{ at } 0 \le \varepsilon_c \le \varepsilon_t \\ f'_{co} + E_{cc}\varepsilon_c \quad \text{at} \quad \varepsilon_t \le \varepsilon_c \le \varepsilon_{cuH} \end{cases} \quad (7)$$

$$\varepsilon_t = \frac{2f'_{co}}{E_c - E_{cc}} \quad (8)$$

where ε_t represents the transition that connects the first linear curve of unconfined concrete with E_c and the second curve of confined concrete with E_{cc} in the stress-strain curve of confined concrete in which the E_c is determined according to [12] as :

$$E_c = 4730\, f_{co}^{'\,0.5}\ (\text{MPa}) \quad (9)$$

$$E_{cc} = \frac{f_{ccH}^{'} - f_{co}^{'}}{\varepsilon_{cuH}} \quad (10)$$

B. Modeling of Concrete (Unconfined)

Authors in [13] developed a model that is adopted in this paper to determine the ultimate unconfined compressive strength of concrete, expressed as:

$$f_{cunc.} = \psi f_{ccu}^{'} \varepsilon_{cr} \frac{1}{(\psi - 1 + \varepsilon_{cr}\,\psi)} \quad (11)$$

$$\varepsilon_{cr} = \frac{\varepsilon_c}{\varepsilon_{co}} \quad (12)$$

$$\psi = \frac{E_c}{E_c - \frac{f_{co}^{'}}{\varepsilon_{co}}} \quad (13)$$

Authors in [14] proposed a model that is adopted in this paper to determine the unconfined concrete strain(ε_{co}):

$$\varepsilon_{co} = (\alpha f_{co}^{'\,2} * \eta\, f_{co}^{'} + 1053)10^6 \quad (14)$$

where $\eta = 29.9$, and $\alpha = -0.0067$

C. Modeling of Steel Reinforcement

The stress-strain curve of steel under tension and compression shows a linear elastic behavior up to the yield point $(\varepsilon_{sy}, f_{sy})$. Therefore, the axial compressive and tensile stresses (f_{si}) at any point can be calculated as:

$$f_{si} = E_s\, \varepsilon_{si} \le f_{sy} \quad (15)$$

where ε_{si} and E_s refer to the axial strain and the elastic modulus of steel at any point, respectively.

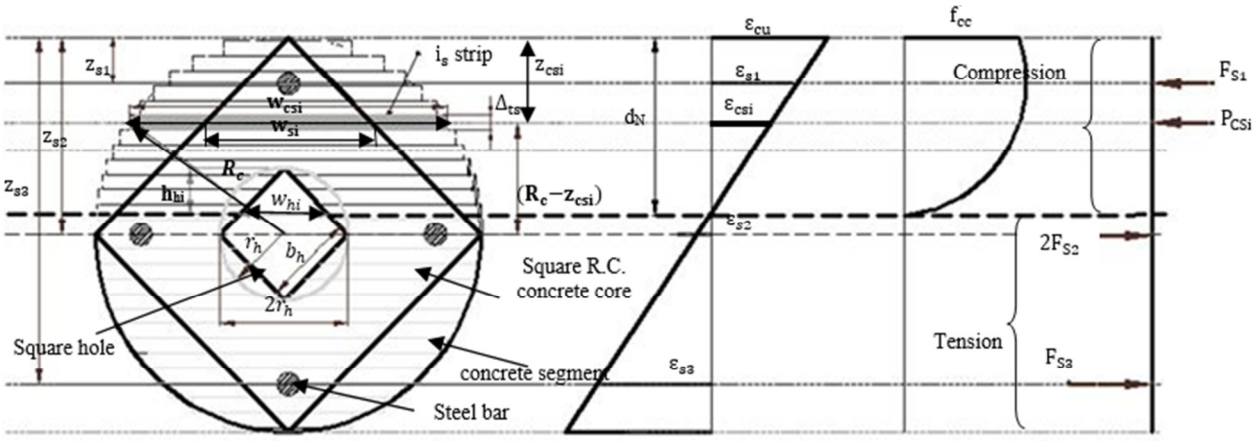

Fig. 2. Stress and strain profile of FRP wrapped shape modified square hollow RC column subjected to bi-axial eccentric loading with (strip method): cross-section, strain distribution, equivalent ultimate concrete stress and forces.

D. Tensile Modeling of FRP

The stress-strain curve of FRP under tensile load is linear elastic up to failure. Therefore, the tensile stress of FRP at any point (f_{Frpi}) can be calculated as:

$$f_{Frpi} = E_{frup}\, \varepsilon_{Frpi} \le f_{frup} \quad (16)$$

E. Theoretical L-M Interactions under Uni-axial and Biaxial Eccentricities.

The cross-sectional area of the concrete column is divided into finite strips with a thickness (Δt) equal to 1 in the current study. This approach is a strip method in which the accuracy of the analysis increases as the strip thickness decreases.

By calculating the internal stresses in each concrete strip using the constitutive models for confined and unconfined concrete, the axial load is determined. The axial stress is multiplied by the effective area of each strip, considering any holes in the cross-section. The total axial load of the entire concrete section is then obtained by summing the axial forces of all the concrete strips. Concrete in the tension zone below the neutral axis is neglected. The assumptions made in the section analysis include the following: steel is embedded within the concrete section, plane sections remain plane during the analysis, a full bond is assumed between the core column and the surrounding concrete segments, and no debonding is considered between the concrete and the FRP.

F. L-M Calculations

The values of Load and Moment (L-M) for any region along the interaction diagram are calculated by the section analysis using the strip method. A linear strain variation is assumed across the cross-section with a maximum value equal to the ultimate concrete compressive strain in the furthest point in the compression part of the section (ε_{cuH})

The axial strain for concrete strip (ε_{csi}) is calculated as:

$$\varepsilon_{csi} = \varepsilon_{cuH} \frac{z_{csi}}{d_N} \quad (17)$$

where (d_N) is the distance from the furthest point in the compression part of the section to the section's neutral axis.

The details of the strip section analysis and strain variation are shown in Figure 2.

To calculate the area of each concrete strip (A_{csi}), the thickness (Δt) is multiplied by the width in which the width of concrete strip w_{si} for the circular cross section is calculated as:

$$w_{si} = 2\sqrt{((R_c)^2 - z_{csi}^2)} \quad (18)$$

To calculate the axial stress for the concrete strip (f'_{csi}), the modified stress-strain model in (7) and (8) was utilized. After determining the stress and strain for each concrete strip, the axial load of the concrete strip (P_{csi}) is calculated as:

$$P_{csi} = f'_{csi} A_{csi} \quad (19)$$

The axial compressive load of concrete (P_c) is calculated by the summation of axial compressive load in each strip as:

$$P_c = \sum_{i=1}^{n} P_{csi} \quad (20)$$

The arm of moment for concrete strip for circular sections (z_{csi}) is calculated as:

$$z_{csi} = R_c - \Delta t\left(i_s - \frac{\Delta t}{2}\right) \quad (21)$$

i_s=1, 2, 3, …, n, where n is the number of concrete strips ($n = \frac{2R_c}{\Delta t}$).

The bending moment of each concrete strip (M_{csi}) is calculated as:

$$M_{csi} = P_{csi}(R_c - z_{csi}) \quad (22)$$

The moment of concrete (M_c) is calculated by the summation of moments in concrete strips as:

$$M_c = \sum_{i=1}^{n} M_{csi} \quad (23)$$

The axial compressive/ tensile strain for main steel bars (ε_{sj}) is determined as:

$$\varepsilon_{sj} = \varepsilon_{cuH}\frac{d_N - z_{sj}}{d_N} \quad (24)$$

where z_{sj} is the distance from the centre of the main steel bar to the centre of the circular concrete section, and j=1,2,3,.. n_s, where n_s is the number of concrete strips.

The axial compressive/axial tensile stress (f_{sj}) for the main steel bar is determined by multiplying the modulus of elasticity of he main steel bar (E_s) by the axial strain (ε_{sj}) as:

$$f_{sj} = E_s \varepsilon_{sj} \leq f_{sy} \quad (25)$$

where f_{sy} represents the yield stress in the steel bars.

$$F_{sj} = A_{sj} f_{sj} \quad (26)$$

The axial load of the main steel bars (F_s) is calculated by the summation of the axial load of all main steel bars as:

$$F_s = \sum_{j=1}^{n_s} F_{sj} \quad (27)$$

The bending moment of each main steel bar (M_{sj}) is:

$$M_{sj} = F_{sj}(R_c - z_{sj}) \quad (28)$$

The bending moment of main steel bars (M_s) is determined by the summation of moments in all main steel bars as:

$$M_s = \sum_{j=1}^{n_s} M_{sj} \quad (29)$$

The load capacity for the specimens is calculated as:

$$P_u = 0.85 P_c + F_s \quad (30)$$

The bending capacity (M_u) for the concrete specimen is determined as:

$$M_u = M_c + M_s \quad (31)$$

It is proposed that the biaxial load and biaxial bending moment are calculated using biaxial eccentricity e_b for symmetrical loading about diagonal axis for the square cross section as:

$$e_b = \sqrt{e_x^2 + e_y^2} \quad (32)$$

To represent the biaxial loading for columns, the cross-section is discretized diagonally for the geometric arrangement of the steel reinforcement. The strip area for the diagonally discretized square cross section is calculated as:

$$A_{si} = w_{si} * \Delta_{ts} \quad (33)$$

$$w_{si} = 2 h_{csi} \quad (34)$$

$$h_{csi} = \begin{cases} Z_{csi}, & Z_{csi} < R_C \\ (2R_c - Z_{csi}), & R_C \leq Z_{csi} \leq 2R_C \end{cases} \quad (35)$$

In this study, the hole has a square cross section; the area of the hole is subtracted with respect to the height of the neutral axis:

$$A_{hi} = w_{hi} * \Delta_{ts} \quad (36)$$

$$w_{hi} = 2 h_{hi} \quad (37)$$

$$h_{hi} = \begin{cases} (Z_{csi} - R_c + r_h), & Z_{csi} < R_C \\ (r_h + R_c - Z_{csi}), & Z_{csi} \geq R_C \end{cases}, \quad (38)$$

where: $r_h = \frac{b_h}{\sqrt{2}}$, $R_C = \frac{b_C}{\sqrt{2}}$.

Equation (38) is applied for the interval when:

$$(R_C - r_h) < Z_{csi} > (R_C + r_h) \quad (39)$$

III. VERIFICATION OF THE THEORETICAL RESULTS WITH THE EXPERIMENTAL RESULTS ADOPTED FROM THE LITERATURE

To examine the validity of the adopted concrete constitutive models within the strip method, a study was used to validate the theoretical analysis of the shape-modified hollow RC columns wrapped with CFRP under various uniaxial load eccentricities, as presented in [4]. Authors in [9] also performed experimental testing, which is adopted herein to verify the theoretical model for the FRP-wrapped square solid RC columns subjected to biaxial eccentric loading.

Authors in [4] tested sixteen concrete specimens to examine the influence of shape modification on the behavior of the hollow RC concrete column wrapped with 2-layers of CFRP sheet under different uniaxial load eccentricities. This study focuses solely on Group HCF in which the specimens were modified into a circular cross section and wrapped with two layers of

CFRP sheets. In this designation, H stands for hollow, C for the modified circular shape, and F for FRP wrapping. The core specimen had a 150 mm x 150 mm section with a 50 mm x 50 mm hole and 800 mm length. After modification, the circular cross section had a 212.12 mm diameter. Each of the specimens reinforced with four steel bars of 12 mm diameter and tied by plain steel ties of 6 mm diameter was placed 60 mm center to center along the specimen's longitudinal axis. The tensile strength of the steel bars and the steel ties were 570 MPa and 478 MPa, respectively. The concrete clear cover was 17mm. The curved segments and the core column were made with the same properties of 40MPa compressive strength concrete, tested according to [15]. The wrapping material was 10 mm width CFRP sheets of 1102 N/mm per (mm unit width) tensile strength, 0.0163 mm/mm axial tensile strain, and elasticity modulus of 67500 N/mm, as reported from the coupon test conducted in [16]. The loading conditions were axial concentricity ($e = 0$), 25 mm uni-axial eccentricity, 50 mm uni-axial eccentricity, and flexural load. Further information is provided in [4].

Authors in [9] tested RC specimens, which had a 135 mm x 135 mm square section with 540 mm length, and were reinforced with four No. 10 steel bars having 550 MPa and 725 MPa yield and ultimate tensile strength, respectively. The main bars were tied with grade 300-6 mm diameter transverse plain steel placed at 150 mm from center to center. The compressive strength of all specimens was ($f'_c = 20$mm). The concrete clear cover was 18.5 mm. The wrapping material was a unidirectional CFRP sheet with manufacturer properties of 0.381 mm thickness, 65.4 GPa tensile modulus, and 1.33% elongation. The specimens were wrapped with one layer of CFRP. A symmetrical eccentricity of $e/b = 0.3$ was applied. The specimen SF-eb was adopted in which S refers to square, F refers to FRP wrapped, and eb refers to biaxial eccentricity. More details are available in [9]. The experimental results and corresponding theoretical results for the uni-axially loaded CFRP wrapped shape modified hollow RC column are depicted in Figure 3. The experimental to theoretical axial compressive load was 1.15, for specimen HCF-0.

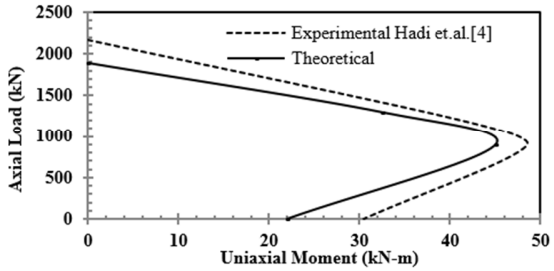

Fig. 3. Theoretical and experimental uniaxial load–moment interaction for CFRP-wrapped hollow RC columns.

The experimental to theoretical axial compressive load and uni-axial bending moment were 0.934 and 1.26, respectively, for specimen HCF-25, and were 0.988 and 1.077, respectively, for specimen HCF-50. The experimental to theoretical uni-axial bending moment was 1.388 for specimen HCF-F. The experimental results and corresponding theoretical results for the bi-axially loaded FRP confined square solid RC columns are as displayed in Figure 4. The experimental to theoretical axial compressive load and corresponding bi-axial bending moment were 1.12 and 1.2, respectively, for specimen SF-eb. According to the results, the adopted stress-strain constitutive models for concrete and the strip method analysis showed reasonable results compared to the counterpart's experimental results, which are convenient to investigate the bi-axial analysis for the CFRP wrapped shape modified hollow.

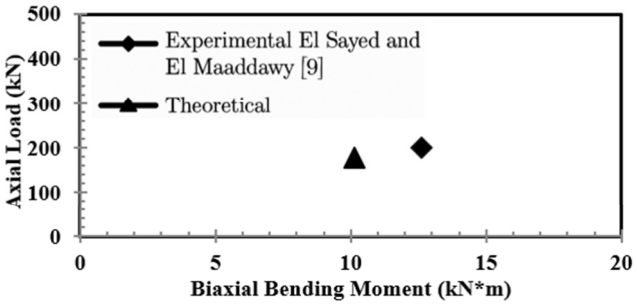

Fig. 4. Theoretical vs. experimental biaxial load-bending moment interactions for CFRP wrapped square solid RC columns.

IV. THEORETICAL ANALYSIS OF BI-AXIALLY LOADED FRP WRAPPED SHAPE MODIFIED SQUARE HOLLOW RC SPECIMENS (PARAMETRIC STUDY).

In this study a reference specimen is proposed to examine the effect of some parameters (concrete strength, number of FRP layers, and hole size) on the axial load and bending moment capacity of the FRP wrapped shape modified square hollow RC specimens under symmetrical biaxial load eccentricities about the diagonal axis. The proposed section is a square specimen with 800 mm height and 150 mm side length. The section has a square hole of 50 x 50mm size. The specimen has concrete compressive strength of 40Mpa and was reinforced with four main steel bars of 12 mm diameter with 570 MPa tensile and compressive yield strength. The main steel bars were tied with 6 mm plain steel of 478 MPa arranged at spaces of 60 mm center to center. The concrete clear cover is 17 mm. The concrete segments have the same properties of/with the square column for the modified specimen. The FRP sheets of 67500 N/mm unit length and 0.0163 mm/mm tensile strain are considered. Two layers are applied for the reference specimen. The details are as portrayed in Figure 1. The theoretical L–M diagram is developed by identifying four principal points corresponding to distinct loading conditions: the pure compression (i.e., no bending), the zero-tension point (where the tensile strain in the steel reinforcement is zero), the balanced failure point (simultaneous yielding in tension and compression), and the pure bending, along with any additional intermediate points considered necessary [17, 18]. The load eccentricities are symmetrical about the diagonal axis and the balance point for the reference specimen is determined at ($e_x = e_y = 42$ mm), while the other point is chosen as ($e_x = e_y = 29$ mm).

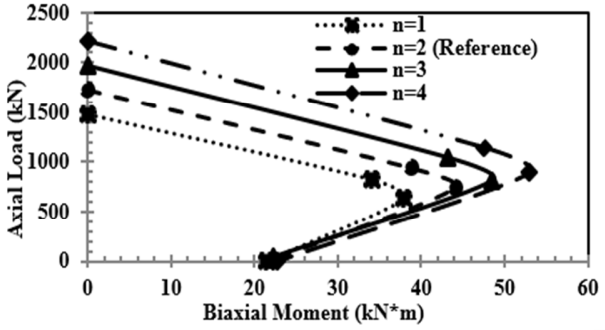

Fig. 5. Biaxial load-bending moment interactions of RC columns wrapped with different number of FRP layers.

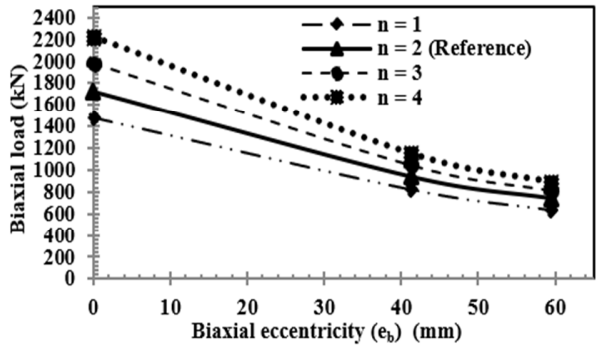

Fig. 6. Influence of number of FRP layers on the biaxial load with increased load eccentricity of the shape modified RC columns.

Figure 5 shows the effect of the number of wrapping FRP layers (1, 2, 3 and 4) on the biaxial compressive load and corresponding biaxial bending moment interactions for the specimens. Figure 5 reveals that the biaxial axial load increases with the increase in the number of wrapping FRP layers. However, the effect of the number of wrapping FRP layers decreases significantly with the increased load eccentricity in terms of the biaxial compressive load, as depicted in Figure 6.

Figure 7 demonstrates that the effect of the number of FRP wrapping layers on the biaxial bending moment increased slightly with the increased eccentricity up to the balance point, and that the effect is insignificant after the balance point. This is due to the reduced confined area of concrete in the compression zone with the increased eccentricity in which the failure mode changes from compression-controlled failure for low eccentricity into tension controlled for high eccentricity.

Figure 8 exhibits the effect of the compressive strength of concrete (30MPa, 35MPa, 40MPa and 45MPa) on the biaxial load and corresponding bending moment interactions for the specimens. For all specimens, the square hollow RC column and the concrete segments are considered to have the same concrete. Figure 8 displays that the biaxial axial load and corresponding biaxial bending moment enhanced with the increased compressive strength of concrete. The effect of compressive strength of concrete decreases slightly with the increased load eccentricity in terms of biaxial axial load, as illustrated in Figure 9.

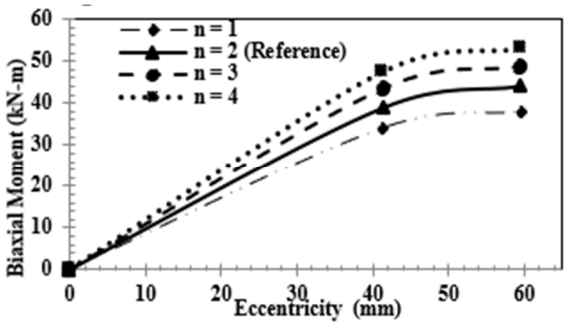

Fig. 7. Influence of number of FRP layers on the biaxial bending moment with increased load eccentricity of the shape modified RC columns.

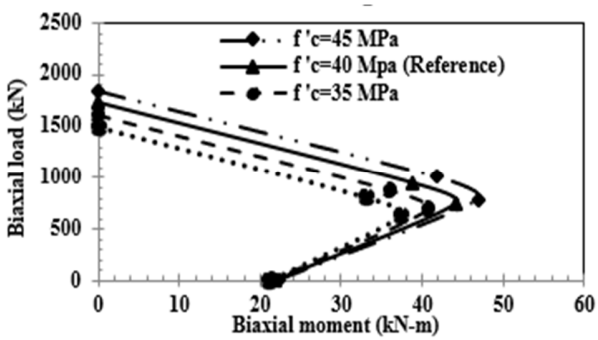

Fig. 8. Biaxial load-bending moment interactions of RC columns wrapped with different concrete strength.

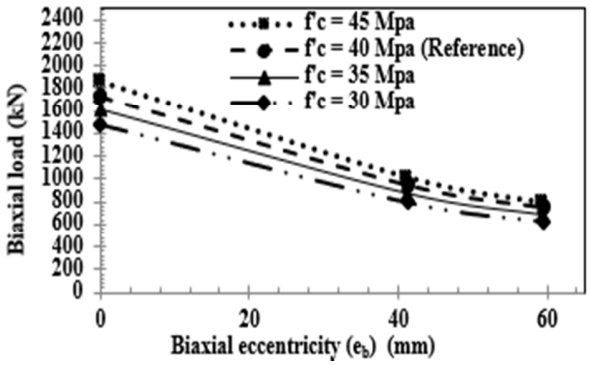

Fig. 9. Influence of concrete strength on the biaxial load with increased load eccentricity of the shape modified RC columns.

Figure 10 shows that the effect of the number of FRP wrapping layers on the biaxial bending moment increased slightly with the increased eccentricity up to the balance point, and that the effect is insignificant after the balance point. This is due to the reduced confined area of concrete in the compression zone in the section with the increased eccentricity, where the failure mode changes from compression-controlled failure for low eccentricity into tension controlled for high eccentricity.

As the hole size increases, its influence on the column's structural performance gradually diminishes. This reduction can be attributed to the simultaneous decrease in both the effective concrete area and the confinement effect provided by the FRP wrapping.

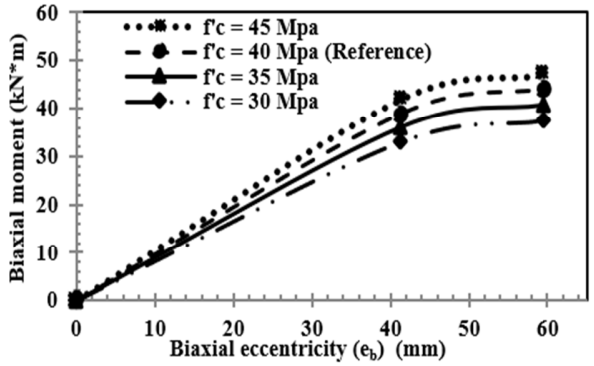

Fig. 10. Influence of concrete strength on the biaxial bending moment with increased load eccentricity of the shape modified RC columns.

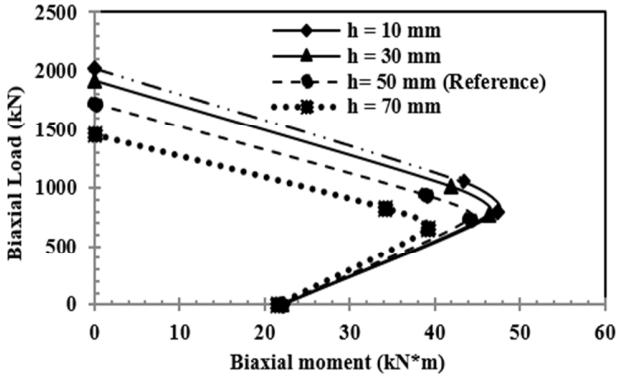

Fig. 11. Biaxial load-bending moment interactions of RC columns wrapped with different hole size.

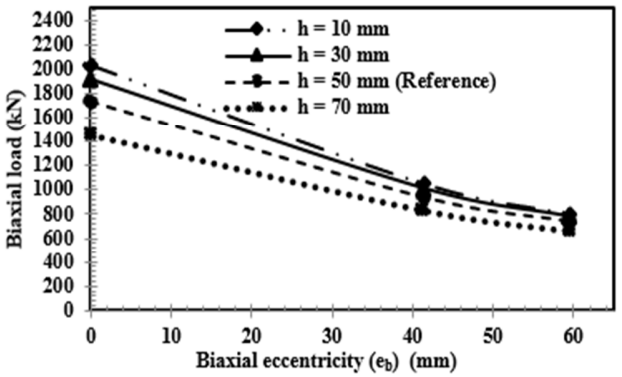

Fig. 12. Influence of hole size on the biaxial load with increased load eccentricity of the shape modified RC columns.

At higher levels of eccentricity, the confined concrete region becomes even smaller, shifting the failure mode progressively toward a tension-controlled behavior. Notably, eccentricity has a greater effect on the impact of the hole size than it does on either the concrete strength or the number of FRP layers. This observation is primarily due to geometric factors: as the square hole enlarges, it increasingly reduces the effective compression zone, particularly as the neutral axis moves further with rising eccentricity. Consequently, the ratio of the hole area to the confined zone becomes larger, leading to reduced confinement efficiency. Moreover, the biaxial load–moment interaction is found to be more sensitive to the number of FRP layers than to the compressive strength of concrete. This is likely due to the enhanced confinement provided by additional FRP layers, which causes the failure mode to shift further toward tension control.

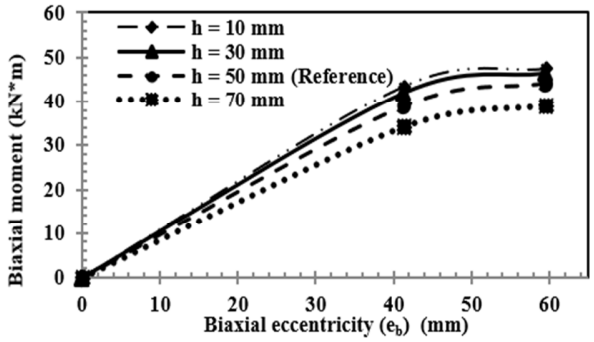

Fig. 13. Influence of hole size on the biaxial bending moment with increased load eccentricity of the shape modified RC columns.

V. CONCLUSIONS

This paper presented a theoretical investigation into the axial load–biaxial moment interaction behavior of square hollow Reinforced Concrete (RC) columns modified into circular sections by the addition of concrete segments and subsequent Fiber Reinforced Polymer (FRP) wrapping, a configuration not previously explored in the literature. The analysis employed a strip method in which the cross-section of the column was divided into several strips, and established constitutive stress–strain models were incorporated. The results showed good agreement with the available experimental data. The findings demonstrated that both shape modification and FRP confinement significantly enhance the load-carrying capacity of hollow RC columns under combined axial and biaxial bending. The efficiency of FRP confinement was observed to increase with a greater number of FRP layers and higher concrete compressive strength. However, this improvement gradually diminished with increasing load eccentricity. Similarly, an increase in the size of the central opening also contributed to improved confinement efficiency, although this positive effect likewise declined at higher eccentricity.

REFERENCES

[1] T.-H. Kim, D.-J. Seong, and H. M. Shin, "Seismic Performance Assessment of Hollow Reinforced Concrete and Prestressed Concrete Bridge Columns," *International Journal of Concrete Structures and Materials*, vol. 6, no. 3, pp. 165–176, Sep. 2012, https://doi.org/10.1007/s40069-012-0015-y.

[2] P. Lignola, A. Prota, G. Manfredi, and E. Cosenza, "Multiscale non-linear analysis of RC hollow piers wrapped with CFRP under shear-type load, " *Construction and Building Materials*, vol. 35, pp. 947–959, Oct. 2012, https://doi.org/10.1016/j.conbuildmat.2012.04.064.

[3] R. Modarelli, F. Micelli, and O. Manni, "FRP-confinement of hollow concrete cylinders and prisms," in *Proceedings of the 7th International Symposium on Fiber Reinforced Polymer Reinforcement of Reinforced Concrete Structures*, 2005, pp. 1029-1046.

[4] M. N. S. Hadi, M. T. Jameel, and M. N. Sheikh, "Behavior of Circularized Hollow RC Columns under Different Loading Conditions," *Journal of Composites for Construction*, vol. 21, no. 5, Oct. 2017, Art. no. 04017025, https://doi.org/10.1061/(ASCE)CC.1943-5614.0000808.

[5] G. P. Lignola, A. Prota, G. Manfredi, and E. Cosenza, "Unified theory for confinement of RC solid and hollow circular columns," *Composites Part B: Engineering*, vol. 39, no. 7, pp. 1151–1160, Oct. 2008, https://doi.org/ 10.1016/j.compositesb.2008.03.007.

[6] Z. H. Abdulghafoor and H. A. Al-Baghdadi, "Static and Dynamic Behavior of Circularized Reinforced Concrete Columns Strengthened with Hybrid CFRP," *Engineering, Technology & Applied Science Research*, vol. 12, no. 5, pp. 9336–9341, Oct. 2022, https://doi.org/10.48 084/etasr.5162.

[7] A. W. Abdulsattar and H. A. Al-Baghdadi, "Circularization Technique for Strengthening of Plain Concrete Short Square Columns Subjected to a Uniaxial Compression Compressive Pressure," *Civil Engineering Journal*, vol. 5, no. 3, pp. 636–648, Mar. 2019, https://doi.org/10. 28991/ cej-2019-03091275.

[8] L. Bisby and M. Ranger, "Axial–flexural interaction in circular FRP-confined reinforced concrete columns," *Construction and Building Materials*, vol. 24, no. 9, pp. 1672–1681, Sep. 2010, https://doi.org/10.10 16. /j.conbuildmat.2010.02.024.

[9] M. El Sayed and T. El Maaddawy, "Analytical model for prediction of load capacity of RC columns confined with CFRP under uniaxial and biaxial eccentric loading," *Materials and Structures*, vol. 44, no. 1, pp. 299–311, Jan. 2011, https://doi.org/10.1617/s11527-010-9628-2.

[10] L. Lam and J. G. Teng, "Strength Models for Fiber-Reinforced Plastic-Confined Concrete," *Journal of Structural Engineering*, vol. 128, no. 5, pp. 612–623, May 2002, https://doi.org/10.1061/(ASCE)0733-9445(2002) 128:5(612).

[11] L. Lam and J. G. Teng, "Design-oriented stress–strain model for FRP-confined concrete," *Construction and Building Materials*, vol. 17, no. 6, pp. 471–489, Sep. 2003, https://doi.org/10.1016/S0950-0618(03)00045-X.

[12] *Building Code Requirements for Structural Concrete and Commentary, ACI 318M-14.2014*, Farmington Hills, MI, USA: American Concrete Institute, 2014.

[13] S. Popovics, "A numerical approach to the complete stress-strain curve of concrete," *Cement and Concrete Research*, vol. 3, no. 5, pp. 583–599, Sep. 1973, https://doi.org/10.1016/0008-8846(73)90096-3.

[14] M. A. Tasdemir, C. Tasdemir, S. Akyüz, A. D. Jefferson, F. D. Lydon, and B. I. G. Barr, "Evaluation of strains at peak stresses in concrete: A three-phase composite model approach," *Cement and Concrete Composites*, vol. 20, no. 4, pp. 301–318, Jan. 1998, https://doi.org/10.101 6/S0958-9465(98)00012-2.

[15] *Methods of testing concrete. Method 9, Determination of the compressive strength of concrete specimens, AS 1012.9-1999*, Sydney, Australia: Standards Association of Australia, 1999.

[16] *Standard Test Method for Determining Tensile Properties of Fiber Reinforced Polymer Matrix Composites Used for Strengthening of Civil Structures, ASTM D7565-10*, West Conshohocken, PA, USA: ASTM International, 2010.

[17] L. C. Bank, *Composites for construction: structural design with FRP materials*, 1st ed. Hoboken, NJ, USA: John Wiley & Sons, 2006.

[18] S. Rocca, N. Galati, and A. Nanni, "Interaction diagram methodology for design of FRP-confined reinforced concrete columns," *Construction and Building Materials*, vol. 23, no. 4, pp. 1508–1520, Apr. 2009, https://doi.org/10.1016/j.conbuildmat.2008.06.010.